

Intravascular origin of metastasis from the proliferation of endothelium-attached tumor cells: a new model for metastasis

A.B. AL-MEHD¹, K. TOZAWA¹, A.B. FISHER¹, L. SHIENTAG², A. LEE² & R.J. MUSCHEL²

¹Institute for Environmental Medicine and ²Department of Pathology and Laboratory Medicine, University of Pennsylvania, 269a John Morgan Building, 3620 Hamilton Walk, Philadelphia, Pennsylvania 19104, USA

Correspondence should be addressed to R.J.M.; email: muschel@mail.med.upenn.edu

Metastasis is a frequent complication of cancer, yet the process through which circulating tumor cells form distant colonies is poorly understood. We have been able to observe the steps in early hematogenous metastasis by epifluorescence microscopy of tumor cells expressing green fluorescent protein in subpleural microvessels in intact, perfused mouse and rat lungs. Metastatic tumor cells attached to the endothelia of pulmonary pre-capillary arterioles and capillaries. Extravasation of tumor cells was rare, and it seemed that the transmigrated cells were cleared quickly by the lung, leaving only the endothelium-attached cells as the seeds of secondary tumors. Early colonies were entirely within the blood vessels. Although most models of metastasis include an extravasation step early in the process¹, here we show that in the lung, metastasis is initiated by attachment of tumor cells to the vascular endothelium and that hematogenous metastasis originates from the proliferation of attached intravascular tumor cells rather than from extravasated ones. Intravascular metastasis formation would make early colonies especially vulnerable to intravascular drugs, and this possibility has potential for the prevention of tumor cell attachment to the endothelium.

We used an established fluorescence microscopic technique to view subpleural endothelia *in situ* in isolated, ventilated and perfused rat and mouse lungs, to observe the behavior of fluorescent tumor cells in the pulmonary circulation². The subpleural vasculature in these intact lungs appeared as a network of capillaries arranged in a honeycomb pattern with pre- and post-capillary vessels interposed (Fig. 1a). Vessels in three dimensions were visible at magnifications up to $\times 1,000$, either using autofluorescence or by specific labeling of the endothelium with DiI-conjugated, acetylated low-density lipoprotein (LDL; refs 2,3)(Fig. 1b).

We injected immunosuppressed (nu/nu) mice intravenously with single-cell suspensions of stable transfectants expressing GFP, derived from the 2.10.10 or HT1080 cell lines. The 2.10.10 cell line is a highly metastatic cell line derived from rat embryo fibroblasts transformed with *ras*^H and *myc* oncogenes^{4,5}. The HT1080 cell line is a metastatic human cell line derived from a fibrosarcoma⁶. We collected the lungs 4–6 hours after the injection of 2.10.10-GFP or HT1080-GFP. Tumor cells were attached to the vascular walls, as shown by intact organ microscopy. Most of the cells of either cell line were attached to the endothelia of pre-capillary arterioles (Fig. 1c), although at early times about 35% of the attached cells were also in the capillaries (Fig. 1d). The percentage of cells in the capillaries decreased with time (Table 1, top). This indicates that the cells were not arrested by capillary trapping, as they were mainly in the pre-capillary arterioles, which have diameters considerably larger than the tumor cells. The cells at these early times did not appear in clumps, but were attached individually (Table 1, middle

and Fig. 1b). Thus, these cells were firmly attached to the blood vessels, as they survived lung clearing for blood removal. Furthermore, they did not move with perfusion during real-time observation.

To verify that the cells were not trapped, we injected either the 2.10.10-GFP or the HT1080-GFP cells into the perfusate of isolated rat lung preparations. Within 10 minutes, most of the cells in the subpleural vessels were immobile and attached to the endothelia of the pre-capillary arterioles (Fig. 1e), although cells were also present in the capillaries (Fig. 1f), similar to the distribution after injection into live animals. In almost all cases, the diameter of the vessel was greater than the diameter of the cells, again indicating that capillary trapping was not the main mechanism leading to retention of the cells in the lung. These experiments also demonstrate that the attachment does not require platelets or other blood elements, as they have been already 'flushed out' from the lung. However, it is still possible that blood components that remain adherent to the endothelial cells can be involved in this interaction.

Because hematogenous metastasis is usually modeled in stages in which the blood-borne cell either attaches to the endothelium or is trapped in the capillary followed by extravasation into the tissue parenchyma, we expected to find frequent extravasation⁷. However, despite an intense search for extravasation, we found

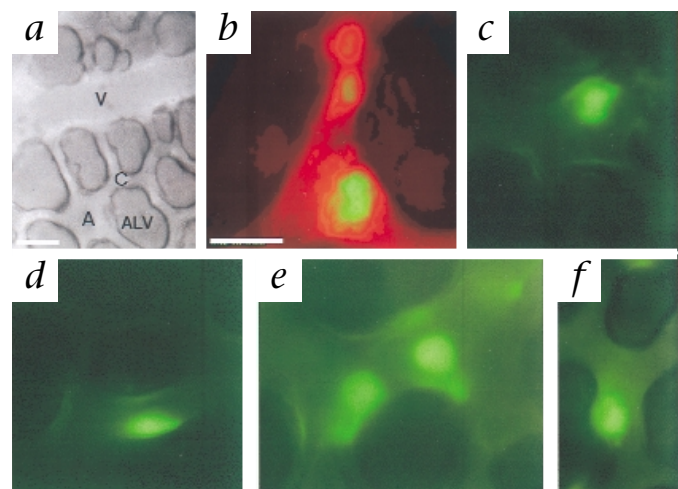


Fig. 1 Localization of tumor cells in the subpleural pulmonary microvessels. **a**, Structure of the subpleural vasculature in the mouse lung. A, arteriole; V, post-capillary venule; C, capillaries; ALV, alveolus. **b**, Fluorescence overlay image of endothelium stained with DiI-acetylated LDL (red) and a GFP-expressing tumor cell (green). **c** and **d**, Endothelium-attached GFP-expressing tumor cells in mouse lung pre-capillary arterioles (c) and in a capillary (d), 4–6 h after intravenous injection. **e** and **f**, Endothelium-attached GFP-expressing tumor cells in a pre-capillary arteriole (e) and in a capillary (f), 10 min after perfusate administration in isolated rat lung. Scale bars represent 50 μm (a) and 32 μm (b–f, shown in b).

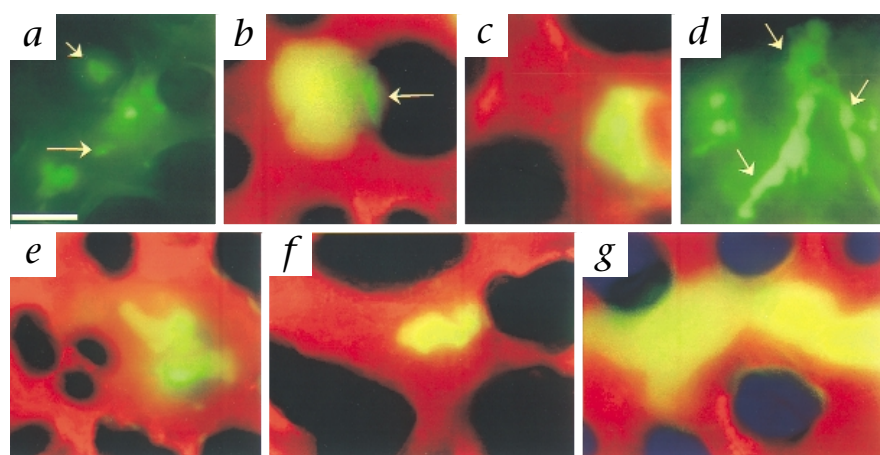


Fig. 2 Fate of tumor cells in the pulmonary circulation. *a* and *d*, Green GFP fluorescence only; *b, c, e-g*, Pseudocolor overlay of DiI-acetylated LDL (red) and GFP (green) fluorescence (yellow, co-localization; black, alveolar space). *a*, Extravasation of a 2.10.10 cell (short arrow) into alveolar space and intravascular tumor cell fragmentation (long arrow). *b*, 2.10.10 cell pseudopodium (arrow) penetrating the vascular wall. The cell is yellow, due to overlay with the endothelium, and the pseudopodium is green as it extends beyond the endothelium into the alveolar space. *c*, HT1080 cell growth in a pre-capillary arteriole. *d*, Intracapillary extension (arrows) of a growing colony (diffuse green background). *e* and *f*, Colony formation by 2.10.10 cells in large pre-capillary arterioles. *g*, Capillary growth of 2.10.10 cells. Scale bars represent 32 μ m (*a, c, d* and *e*, shown in *a*) and 10 μ m (*b* and *g*, shown in *g*).

tumor cell transmigration out of the vasculature only rarely (Table 1, middle). Before 24 hours, less than 2% of all cells found after intravenous injection were in the extravascular space (Fig. 2*a*). We never found any extravasated 2.10.10 cells beyond 24 hours after injection or HT1080 cells beyond 48 hours after injection. Although extravasation was rare, penetration of the vascular wall by pseudopodia occurred more often (Fig. 2*b*). The basement membrane of the vessels seemed to be breached by pseudopodia from tumor cells, and there were occasional intravascular green cell fragments (Fig. 2*a*) in the interstitium or within alveoli, but intact cells did not persist extravascularly for more than 48 hours. We confirmed the location of the endothelial cell margins by labeling with DiI-acetylated LDL (ref. 3).

Given the absence of tumor cells in the parenchyma, we sought to determine the location of cells that gave rise to metastatic nodules. At 48 hours for 2.10.10 cells and at 72 hours for HT1080 cells, colonies of GFP-expressing cells could be identified. Every colony was contained entirely within the vascular channels (Table 1, bottom and Fig. 2*c-g*). These colonies are unlikely to be emboli, as at earlier times there were mainly single cells and no clumps or clusters. Because all of the cells seen by intact organ microscopy were attached to the endothelium and were within the vascular channels, cell division must have been occurring within the pulmonary vasculature. At later times, as the colonies grew larger, the tumor cells seemed to be growing as strings into the capillaries from their primary location within larger vessels (Fig. 2*d*). Strings of cells were never present in the capillaries at times earlier than 48 hours.

electron microscopy methods used in previous studies only allowed localization of occasional tumor cells that happened to be present in the sectional plane. Most tumor cells in a tissue easily escape detection because of the inability to visualize whole cells and blood vessels in three dimensions using these thin-section methods. Determining the relationship between the tumor cells and vascular margins also suffers considerably because of the same problem. The difficulty is accentuated by the absence of pressure in the vascular channels that causes them to collapse. Nonetheless, some reports have demonstrated the presence of intravascular colonies with these methods¹²⁻¹⁴. In contrast, the use of fluorescence microscopy in a translucent intact organ (lung) allows the determination of position of many GFP-labeled tumor cells with high three-dimensional accuracy. Combined with specific fluorescence labeling of endothelial cells, this method allows precise, long-term visual monitoring of

Previous observations of the fate of metastatic cells within the blood stream are consistent with our results, in that the introduction of radioactively tagged tumor cells into the circulation led to rapid clearance from the blood with most of the radioactivity being sequestered in the lungs, consistent with attachment^{8,9}. Previous electron microscopic examination of tumor cell metastases is consistent with our observation of pseudopodia ('invadopodia') extending beneath the endothelial cell basement membrane^{10,11}. Although the 'mainstream' view is that circulating metastatic cells must extravasate before proliferating into colonies, other models have been proposed in which the colonies arise within the vasculature^{1,12}. There has been similar controversy about whether the circulating tumor cells are trapped in the capillaries because of size restrictions or adhere to the pulmonary endothelium. Such controversies could have arisen from extrapolation of two-dimensional data (observations from thin sections) into a three-dimensional concept (relationship of whole cells to vessel lumen). The light and

Table 1 Fate of tumor cells in the pulmonary circulation after intravenous injection

	4-6 h	24 h	48 h	72 h
	Percent of cells in capillaries (total number of observed cells)			
HT1080-GFP	35 \pm 22 (394)	20 \pm 2.5 (177)	9 \pm 3.5 (136)	(247) ^a
2.10.10-GFP	35 \pm 9 (451)	12 \pm 3 (288)	(207) ^a	(>300) ^a
	Percent extravasated (total number of observed cells)			
HT1080-GFP	1.5 (394)	1.1 (177)	0 (136)	0 (247)
2.10.10-GFP	0.44 (451)	0 (288)	0 (207)	0 (>300)
	Number of colonies with \geq 5 cells (number of cells/colony)			
HT1080-GFP	0	0	0	21 (5-15); 4 (>15)
2.10.10-GFP	0	0	28 (5-15); 41 (>15)	3 (7-15); 15 (>15)

Lungs isolated from mice injected intravenously were examined intact by fluorescence microscopy (times after injection, above table); $n = 3-4$ mice at each time point for each cell line. Green-fluorescing cells were counted in the subpleural vasculature. Top, Localization of attached tumor cells in the subpleural vessels. Capillaries were defined as vessels having a diameter of about 10 μ m; most cells were in pre-capillary arterioles. ^aAs colonies formed and cells grew into capillaries, it was not possible to count the number of cells growing into the capillaries. Middle, Localization of cells with respect to vascular margins, defined by the presence of continuous endothelial lining shown by autofluorescence or labeling with DiI-acetylated LDL. Multi-plane z-axis imaging of a horizontally oriented vessel was used to determine if a tumor cell that seemed to be inside a vessel was actually above, inside or below it. For vessels that appeared as in a cross-section, visualization covered the length of the cell along the z-axis. Bottom, Early colony formation in subpleural vessels. Preparations were examined for clumps of cells; a colony was defined as a clump of at least five cells in contact with each other. We attempted to count the number of cells in each clump, although sometimes the cells were close together, making it difficult to distinguish each cell precisely.

spatio-temporal relationships between tumor and endothelial cells.

The idea of an extravascular origin of metastasis is most strongly supported by intravital observations in the liver, where frequent extravasation of tumor cells has been shown with low-resolution, analog video microscopy^{1,15}. However, this may be related to the sinusoidal nature of the vascular channels with interrupted endothelial lining in the liver, which facilitates easy passage of cells into the tissue parenchyma. Nonetheless, metastatic colonies in the liver seem to arise within the blood vessels¹⁶. Another theoretical rationale for the extravascular model is based on the premise that loss of cell contact with substrate leads to accelerated death in circulation and prevents intravascular growth^{17,18}. Although that may be true for non-tumor cells, anchorage-independent growth of tumorigenic cells in suspension and metastatic cells *in vivo* has been shown^{19,20}. Furthermore, our observation that colonies arose from attached cells indicates that endothelial attachment not only determines the physical site of metastasis, but also provides the necessary anchorage that facilitates cell proliferation.

Based on these observations, we now suggest a new model for pulmonary metastasis in which endothelium-attached tumor cells proliferate intravascularly and give rise to metastatic foci without the requirement for extravasation. Although extravasation can occur, the transmigrated cells in the interstitium or alveoli are quickly cleared in the lung. Proliferation by metastatic colonies seems to originate from intravascular cells, and at early stages, micrometastases are contained entirely within the vasculature. With time, the colonies would outgrow the vessels they were in and destroy the vascular walls. This model identifies several targets for potential therapeutic intervention, including attachment to the endothelium and inhibition of proliferation within the blood vessels.

Methods

Intact organ microscopy. We used an established intact organ microscopy technique to observe and image fluorescently labeled tumor cells and capillary endothelial cells *in situ* in isolated, ventilated, blood-free rat and mouse lungs in real time using an epifluorescence microscope². For lung isolation, the animal was anesthetized, a tracheostomy was done and artificial ventilation was started through a cannula. The abdomen was opened and the animal was exsanguinated by transection of major abdominal vessels. A cannula was inserted into the main pulmonary artery through a puncture in the right ventricle and another was inserted into the left atrium. The lung was cleared of blood by gravity perfusion through the pulmonary artery with an artificial medium (Kreb-Ringer bicarbonate buffer with 5% dextran and 10 mM glucose, pH 7.4). The 'flow-through' perfusate left the lung through the left atrial cannula. Once the lung became visibly cleared of blood, the heart-lung preparation was dissected *en bloc* and placed in a specially designed Plexiglas chamber with ports for the tracheal, pulmonary and left atrial cannulae. The cardiovascular ports were connected to a peristaltic pump that recirculated perfusate through the pulmonary vascular bed. The lung rested on a coverslip window at the bottom of the chamber with the posterior surface of the lung touching the coverslip. The lung was ventilated throughout the experiment with 5%CO₂ in air except during imaging. The preparation was physiologically stable for up to 8 h. The integrity of the preparation was continuously monitored by online measurements of intratracheal and pulmonary artery perfusion pressures. The subpleural vasculature of the lungs was directly visualized in these conditions using high-power magnification by epifluorescence microscopy (Nikon Diaphot TMD; Nikon, Mellville, New York) with autofluorescence of lung tissue or an appropriate endothelial cell label. The focal range of a 60× objective allowed clear visualization of up to 30 μm in depth, covering the full thickness of the subpleural vessels. Endothelial cells in the subpleural vasculature were positively identified by labeling with DiI-acetylated LDL (Molecular Probes, Eugene, Oregon) added to the perfusate, at a concentration of 100 μg per g lung wet weight. Perfusion with a peristaltic pump at 10 ml/min for rat lung and 2 ml/min for mouse lung resulted in homogenous recruitment of more than 99% of capillaries in the dependent regions of the lung, which were viewed with our system. Studies with fluorescently labeled red blood cells confirmed the uniformity of perfusate flow

throughout the subpleural vascular network. The diameter of the capillaries was variable with perfusion pressure and averaged about 10 μm at our regular perfusion rates. To observe and image fluorescently labeled tumor cells and capillary endothelial cells *in situ*, we used the following two methods: we isolated the lungs from 4- to 6-week-old female nude mice that had been injected into the tail vein with 2 × 10⁶ HT1080-GFP or 2.10.10-GFP cells, or we administered 1.5 × 10⁷ cells into the perfusate of isolated Sprague-Dawley rat lungs. The subpleural vessel autofluorescence and GFP-expressing cells were visualized with an HQ41001 FITC Filter (excitation, 480 ± 20 nm; dichroic, 505 nm long pass; emission, 535 ± 20 nm); endothelial labeling with DiI acetylated LDL was visualized with an HQ412002b TRITC Filter (excitation, 545 ± 15 nm; dichroic, 565 nm long pass; emission, 610 nm ± 37.5) (Chroma Technology, Brattleboro, Vermont). Images were acquired with a Hamamatsu ORCA-100 12-bit digital camera and MetaMorph Imaging software (Universal Imaging, West Chester, Pennsylvania).

Cell culture. 2.10.10 or HT1080 cells were transfected with an expression vector for GFP (pEGFP-1; Clontech, Palo Alto, California). Using flow cytometry, the brightest fluorescent cells above the 95th percentile were sorted and cloned. Cells are maintained by selection with 200 μg/ml geneticin (Life Technologies).

Acknowledgments

We thank Y. Dong and M. Meuler for technical assistance and W.G. Mckenna and E.J. Bernhard for reading the manuscript. This work was supported by a Parker B. Francis fellowship (A.B.A.), National Institutes of Health RO1 CA46830-09 (R.J.M.) and SCOR P50-HL60290 (A.B.F.), and a Merck Research fellowship (L.S.).

RECEIVED 9 SEPTEMBER; ACCEPTED 8 OCTOBER 1999

- Luzzi, K.J. *et al.* Multistep nature of metastatic inefficiency: dormancy of solitary cells after successful extravasation and limited survival of early micrometastases. *Am. J. Pathol.* **153**, 865–873 (1998).
- Al-Mehdi, A. B. *et al.* Endothelial NADPH oxidase as the source of oxidants with lung ischemia or high K⁺. *Circ. Res.* **83**, 730–737 (1998).
- Voyta, J.C., Via, D.P., Butterfield, C.E. & Zetter, B.R. Identification and isolation of endothelial cells based on their increased uptake of acetylated-low density lipoprotein. *J. Cell Biol.* **99**, 2034–2040 (1984).
- Bernhard, E.J., Gruber, S.B. & Muschel, R.J. Direct evidence linking expression of matrix metalloproteinase 9 (92-kDa gelatinase/collagenase) to the metastatic phenotype in transformed rat embryo cells. *Proc. Natl. Acad. Sci. USA* **91**, 4293–4297 (1994).
- Hua, J. & Muschel, R.J. Inhibition of matrix metalloproteinase 9 expression by a ribozyme blocks metastasis in a rat sarcoma model system. *Cancer Res.* **56**, 5279–5284 (1996).
- Frisch, S.M. *et al.* Adenovirus E1A represses protease gene expression and inhibits metastasis of human tumor cells. *Oncogene* **5**, 75–83 (1990).
- Liotta, L.A., Steeg, P.S. & Stetler-Stevenson, W.G. Cancer metastasis and angiogenesis: an imbalance of positive and negative regulation. *Cell* **64**, 327–336 (1991).
- Fidler, I.J. Metastasis: quantitative analysis of distribution and fate of tumor emboli labeled with ¹²⁵I-5-iodo-2'-deoxyuridine. *J. Natl. Cancer Inst.* **45**, 773–782 (1970).
- Fidler, I.J. & Nicolson, G.L. Brief communication: Organ selectivity for implantation survival and growth of B16 melanoma variant tumor lines. *J. Natl. Cancer Inst.* **57**, 1199–1202 (1976).
- Chen, W.T. Proteolytic activity of specialized surface protrusions formed at rosette contact sites of transformed cells. *J. Exp. Zool.* **251**, 167–185 (1989).
- Crissman, J.D., Hatfield, J., Schaldenbrand, M., Sloane, B.F. & Honn, K.V. Arrest and extravasation of B16 amelanotic melanoma in murine lungs. A light and electron microscopic study. *Lab. Invest.* **53**, 470–478 (1985).
- Roos, E., Dingemans, K.P. Mechanisms of metastasis. *Biochim. Biophys. Acta.* **560**, 135–166 (1979).
- Dingemans, K.P. Behavior of intravenously injected malignant lymphoma cells. A morphologic study. *J. Natl. Cancer Inst.* **51**, 1883–1895 (1973).
- Lapis, K., Paku, S., Liotta, L.A. Endothelialization of embolized tumor cells during metastasis formation. *Clin. Exp. Metastasis* **6**, 73–89 (1988).
- Hangan, D. *et al.* Integrin VLA-2 (α₂β₁) function in postextravasation movement of human rhabdomyosarcoma RD cells in the liver. *Cancer Res.* **56**, 3142–3149 (1996).
- Scherbarth, S. & Orr, F.W. Intravital videomicroscopic evidence for regulation of metastasis by the hepatic microvasculature: effects of interleukin-1α on metastasis and the location of B16F1 melanoma cell arrest. *Cancer Res.* **57**, 4105–4110 (1997).
- Boudreau, N., Sympson, C.J. & Werb, Z., Bissell, M.J. Suppression of ICE and apoptosis in mammary epithelial cells by extracellular matrix. *Science* **267**, 891–893 (1995).
- Frisch, S.M. & Francis, H. Disruption of epithelial cell-matrix interactions induces apoptosis. *J. Cell Biol.* **124**, 619–626 (1994).
- Nikiforov M.A. *et al.* p53 modulation of anchorage independent growth and experimental metastasis. *Oncogene* **13**, 1709–1719 (1996).
- Hauser, P.J., Agrawal, D. & Pledger, W.J. Primary keratinocytes have an adhesion dependent S phase checkpoint that is absent in immortalized cell lines. *Oncogene* **17**, 3083–3092 (1998).